

Thermoelectric properties of individual electrodeposited bismuth telluride nanowires

Jianhua Zhou

Department of Mechanical Engineering, The University of Texas at Austin, Austin, Texas 78712

Chuangui Jin

Hefei National Laboratory for Physical Science at Microscale, Department of Materials Science and Engineering, University of Science and Technology of China, Hefei 230026, China

Jae Hun Seol

Department of Mechanical Engineering, The University of Texas at Austin, Austin, Texas 78712

Xiaoguang Li

Hefei National Laboratory for Physical Science at Microscale, Department of Materials Science and Engineering, University of Science and Technology of China, Hefei 230026, China

Li Shi^{a)}

Department of Mechanical Engineering & Center for Nano and Molecular Science and Technology, Texas Materials Institute, The University of Texas at Austin, Austin, Texas 78712

(Received 13 June 2005; accepted 2 August 2005; published online 21 September 2005)

For an electrodeposited bismuth telluride ($\text{Bi}_x\text{Te}_{1-x}$) nanowire from one batch with x found to be about 0.46, the Seebeck coefficient (S) was measured to be 15%–60% larger than the bulk values at temperature 300 K. For four other nanowires from a different batch with $x \approx 0.54$, S was much smaller than the bulk values. The electrical conductivity of the nanowires showed unusually weak temperature dependence and the values at 300 K were close to the bulk values. Below 300 K, phonon-boundary scattering dominated phonon-phonon Umklapp scattering in the nanowires, reducing the lattice thermal conductivity. © 2005 American Institute of Physics.

[DOI: 10.1063/1.2058217]

The energy efficiency of thermoelectric (TE) refrigerators and power generators is limited by the thermoelectric figure of merit (ZT) defined as $ZT \equiv S^2\sigma T/\kappa$, where S is the Seebeck coefficient, σ is the electrical conductivity, κ is the thermal conductivity, and T is the absolute temperature. Further, $\kappa = \kappa_e + \kappa_p$, where κ_e is the electron contribution and κ_p is the phonon contribution to κ . During the past fifty years, bismuth telluride alloys have remained the bulk materials with the highest ZT close to unity at $T=300$ K.^{1–3} ZT needs to be higher than 3 for TE refrigerators to be as efficient as chlorofluorocarbon-based units. It has been suggested that ZT can be increased in low-dimension nanostructures because $S^2\sigma$ can be increased by high electronic density of states near the Fermi level and κ can be suppressed by phonon-boundary scattering and modification of phonon dispersion.^{4–6} Recently, there have been reports on the growth of thin-film superlattices^{7,8} and nanostructured bulk alloys⁹ with improved ZT .

Very high ZT values have been predicted in Bi-based⁴ and III-V¹⁰ nanowires. The ZT of these nanowires have not been obtained in previous measurements.^{11–13} In this letter, we report measurement results of S , σ , κ , and ZT of bismuth telluride ($\text{Bi}_x\text{Te}_{1-x}$) nanowires. The results reveal effects of surface scattering and chemical composition on the TE properties.

Two batches of $\text{Bi}_x\text{Te}_{1-x}$ nanowires were deposited in the nanopores of anodized alumina membranes using an electrochemical deposition method.¹⁴ It was revealed by high-

resolution transmission electron microscopy (HRTEM) measurements that these nanowires were single crystalline, and the growth direction was $\langle 11\bar{2}0 \rangle$, perpendicular to the c axis. During the deposition, the Bi-to-Te atomic ratio in the electrolytes was 2 to 3 for the first batch and 1 to 1 for the second batch. An energy dispersive spectrometer (EDS) of an HRTEM was used to find that the Bi-to-Te ratio of one nanowire from the first batch was 46% to 54%. For four nanowires from the second batch, the average EDS-obtained atomic fraction is 54% of Bi and 46% of Te with a standard deviation of 4.2%.

We have measured the TE properties of the nanowires shown in Table I. Except for sample 2 and sample 3, the measurements were conducted using a suspended microdevice¹⁵ shown in the scanning electron micrograph (SEM) of Fig. 1. For improving the electrical and thermal contacts, a dual-beam SEM and focused ion beam (FIB) system was used to deposit two short platinum (Pt) lines on top of the contacts between the nanowire and the two Pt electrodes on the membranes, which were used to measure S . After measuring S and κ , we deposited two additional short Pt lines to connect the nanowire with the two Pt serpentine lines on the membranes for measuring the four-probe electrical resistance of the nanowire. We avoided imaging the sus-

TABLE I. Diameter (d) of the nanowires.

Sample	1 (2 wires)	2	3	4	5 (2 wires)	6	7	8
Batch	1	1	1	2	2	2	2	2
d (nm)	100 (100)	57.5	43.5	81	120 (80)	75	81	67

^{a)} Author to whom correspondence should be addressed; electronic mail: lishi@mail.utexas.edu

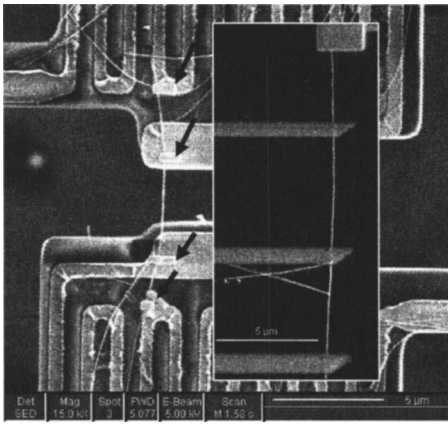


FIG. 1. SEM of a $\text{Bi}_x\text{Te}_{1-x}$ nanowire trapped on the two suspended membranes of the measurement device. Four Pt lines were deposited locally on the nanowire, as labeled by the arrows. The inset is the SEM of another $\text{Bi}_x\text{Te}_{1-x}$ nanowire deposited on an oxidized silicon wafer and contacted by four Pt lines.

pendent segment of the nanowire with either ion-beam or high-magnification SEM in order to prevent sample damage or contamination. After the FIB deposition, we avoided imaging the sample with either the electron or ion beam to prevent converting the residual precursor gas into a conducting layer on the sample. For samples 2 and 3, the nanowire was deposited on an oxidized silicon wafer, and four Pt electrodes were patterned on the nanowire by FIB deposition. For sample 2 shown in the inset of Fig. 1, there was no electrical connection between any two adjacent Pt electrodes after a 100 nm wide cut was made by FIB on the nanowire between the two electrodes, suggesting that the FIB deposition did not cause current leakage.¹⁶ For four-probe resistance measurements, the voltage drop across the two middle electrodes was measured when a current was supplied between the two outer electrodes, where Peltier cooling or heating occurred. Due to heat leakage from the nanowire to the substrate under the segment between an outer electrode and the adjacent middle electrode, the Peltier effects caused a negligible temperature difference and Seebeck voltage between the two middle electrodes.

For sample 1, the obtained S in Fig. 2 was positive, indicating that the nanowire was p -type. The value of $260 \mu\text{V}/\text{K}$ at $T=300 \text{ K}$ was 60% higher than that for bulk $\text{Bi}_{0.46}\text{Te}_{0.54}$ crystal, and 15% higher than that of Bi_2Te_3 , which was found to have the largest S for p -type $\text{Bi}_x\text{Te}_{1-x}$ bulk crystals.¹ For the other nanowires from the second batch, S was negative, suggesting electron-like majority carriers. Among the reported bulk crystals, $\text{Bi}_{0.485}\text{Te}_{0.515}$ with the atomic ratio closest to the second batch was found to

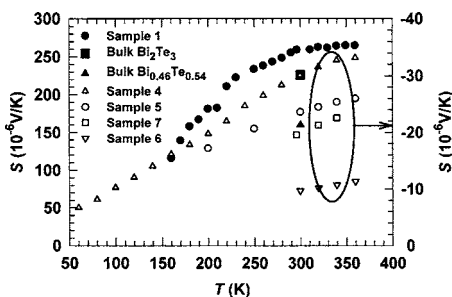


FIG. 2. Seebeck coefficient as a function of temperature. The left Y axis is for filled symbols and the right Y axis is for open symbols.

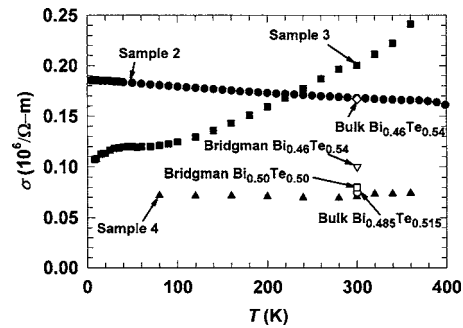


FIG. 3. Electrical conductivity of the nanowires (filled symbols) and bulk crystals (open symbols) as a function of temperature.

have a positive $S=138 \mu\text{V}/\text{K}$,¹ much higher than those for the nanowires from the second batch. While S for sample 1 showed nonlinear T dependence, the observed S of the samples from the second batch exhibited linear T dependence similar to the diffusion S of a metal. As a comparison, bulk $\text{Bi}_x\text{Te}_{1-x}$ crystals is p -type for $x>0.37$, n -type for $x<0.37$, and bulk $\text{Bi}_{0.485}\text{Te}_{0.515}$ is highly p -doped.¹⁷

The σ values obtained from the four-probe resistance measurements are shown in Fig. 3 together with the reported values for $\text{Bi}_{0.46}\text{Te}_{0.54}$ and $\text{Bi}_{0.485}\text{Te}_{0.515}$ bulk crystals. The σ values at $T=300 \text{ K}$ of samples 2 and 3 were close to the value for bulk $\text{Bi}_{0.46}\text{Te}_{0.54}$ and were about two times higher than that for the Bridgman-type $\text{Bi}_{0.46}\text{Te}_{0.54}$ single crystals.¹⁷ While the bulk σ decreases approximately linearly with increasing T due to increased electron-phonon scattering, the σ of the nanowires showed very weak T dependence. For sample 2, the decrease of σ with increasing T was somewhat similar to but at a much smaller slope than the bulk behavior. Although the smaller slope can be attributed to a surface-scattering dominated electron mean free path that only weakly depends on T , the σ value at 300 K of sample 2 was not reduced by surface scattering. For sample 3, σ increased slightly with T . This behavior is somewhat similar to that of a nondegenerate semiconductor, for which an increase of the carrier concentration can lead to an increased σ with T . Additionally, the presence of local defects or conduction barriers in the nanowire can lead to the increased σ with T .

The σ of sample 4 from the second batch was almost independent of T . The value at 300 K was close to those for bulk $\text{Bi}_{0.485}\text{Te}_{0.515}$ crystal and Bridgman-type $\text{Bi}_{0.50}\text{Te}_{0.50}$ single crystals.¹⁷

The thermal conductivity of the three samples from the first batch was not obtained, and only the thermal conductivity (G) was obtained for sample 1. The thermal conductivity of four samples from the second batch has been measured, and the results are shown in Fig. 4 with the obtained G of sample 1.

For bulk Bi_2Te_3 , κ reaches a maximum value at $T<75 \text{ K}$, decreases from $T=75 \text{ K}$ to a minimum at $T\approx 270 \text{ K}$ due to phonon-phonon Umklapp scattering.¹⁸ For sample 1, G increased with T and approached a maximum value at $T>350 \text{ K}$. The shift of the maximum G to high T suggests that phonon-boundary scattering dominated phonon-phonon Umklapp scattering for $T<300 \text{ K}$. For sample 4, κ increased with T and reached a peak value at $T\approx 340 \text{ K}$. Although the peak value revealed an increasing effect of the Umklapp process at high temperatures, phonon-boundary scattering was the dominant scattering process for $T<300 \text{ K}$. For sample 8, the κ versus T curves is approxi-

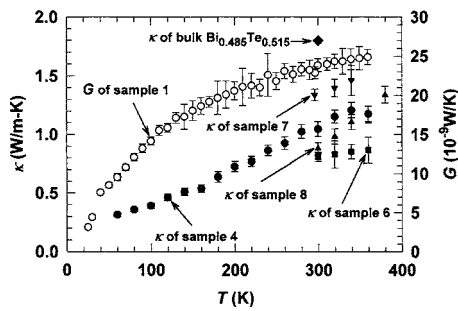


FIG. 4. Thermal conductivity (filled symbols) or thermal conductance (open symbols) as a function of temperature.

mately linear between 300 and 380 K, indicating a large effect of phonon-boundary scattering in this nanowire with the smallest diameter. Although this result may indicate that phonon-boundary scattering could reduce κ more in smaller nanowires, a monotonic decrease of κ with decreasing d was not revealed by Fig. 4, likely due to different surface roughness of different nanowires.

The κ values at $T=300$ K of the nanowires were 28%–57% lower than those for bulk $\text{Bi}_{0.485}\text{Te}_{0.515}$ crystals. We could not find the κ values for bulk $\text{Bi}_x\text{Te}_{1-x}$ crystals with the same x as for the second batch. For the bulk crystals, κ decreased with increased Bi concentration in the range between 41.5% and 48.5%.¹⁷ It is possible that κ is lower for bulk $\text{Bi}_{0.54}\text{Te}_{0.46}$ crystal than for bulk $\text{Bi}_{0.485}\text{Te}_{0.515}$ crystal.

The κ_p and κ_e of sample 4 have been calculated according to the Wiedemann-Franz law with the Lorenz number $L=2.44 \times 10^{-8} \text{ W } \Omega/\text{K}^2$. The calculated κ_p to κ_e ratio was 1.02 at $T=300$ K. This ratio is 2.39 for bulk $\text{Bi}_{0.485}\text{Te}_{0.515}$ crystal and 1.17 for bulk Bi_2Te_3 crystal if the same L value is used.^{2,17} The obtained κ_p at $T=300$ K of sample 4 was 60% lower than that of bulk $\text{Bi}_{0.485}\text{Te}_{0.515}$; while the σ and κ_e at $T=300$ K of the nanowire was only 5.6% lower than that of bulk $\text{Bi}_{0.485}\text{Te}_{0.515}$. The large difference in the reductions in κ_p and σ can have two possible origins. First, the de Broglie wavelength (λ_e) of electrons in these semiconductor nanowires is about 10 nm; while the dominant phonon wavelength (λ_{ph}) is below 1 nm. For a surface roughness (r) on the order of 1 nm, the Rayleigh scattering cross section is proportional to $(r/\lambda)^4$ and much smaller for electrons than for phonons. Hence, the surface roughness may reduce κ_p to a much larger extent than the reduction in σ . Because the atomic ratio of the nanowire is different from that of the bulk crystal used for comparison, however, we cannot rule out the

possibility that an increase of x from 0.485 for the bulk to 0.54 for the nanowire can cause a larger reduction in κ_p than in σ , although σ was found to be reduced more than κ_p when x was increased from 0.4 to 0.485 for the bulk crystals. Additionally, for this nanowire from the second batch, ZT calculated from the obtained S , σ , and κ increased with T and was about 0.02 at $T=300$ K, very low due to the low S for this atomic ratio.

For $\text{Bi}_x\text{Te}_{1-x}$ nanowires from the first batch with $x \approx 0.46$, we found that the S was 15%–60% higher than, and the σ was close to, the corresponding bulk values. We also observed signatures of increased phonon-boundary scattering that should reduce the lattice thermal conductivity. This evidence suggests that high ZT can potentially be obtained in $\text{Bi}_x\text{Te}_{1-x}$ nanowires with an optimized atomic ratio.

Three of the authors (J.Z., J.S., and L.S.), are supported by the US Office of Naval Research (Program manager: Dr. M. E. Gross) and the US National Science Foundation. Two of the authors (C.J. and X.L.), are supported by the Natural Science Foundation of China.

¹D. M. Rowe, *CRC Handbook of Thermoelectrics* (CRC Press, Boca Raton, FL, 1995).

²G. S. Nolas, J. Sharp, and H. J. Goldsmid, *Thermoelectrics: Basic Principles and New Materials Development* (Springer, Berlin, 2001).

³G. Mahan, B. Sales, and J. Sharp, *Phys. Today* **50**, 42 (1997).

⁴Y. Lin, X. Sun, and M. S. Dresselhaus, *Phys. Rev. B* **62**, 4610 (2000).

⁵G. Chen and A. Shakouri, *J. Heat Transfer* **124**, 242 (2002).

⁶A. Balandin and K. L. Wang, *Phys. Rev. B* **58**, 1544 (1998).

⁷R. Venkatasubramanian, E. Siivola, T. Colpitts, and B. O'Quinn, *Nature (London)* **413**, 597 (2001).

⁸T. C. Harman, P. J. Taylor, M. P. Walsh, and B. E. LaForge, *Science* **297**, 2229 (2002).

⁹F. K. Hsu, S. Loo, F. Guo, W. Chen, J. S. Dyck, C. Uher, T. Hogan, E. K. Polychroniadis, and M. G. Kanatzidis, *Science* **303**, 818 (2004).

¹⁰N. Mingo, *Appl. Phys. Lett.* **84**, 2652 (2004).

¹¹Y. Lin, S. B. Cronin, O. Rabin, J. Y. Ying, and M. S. Dresselhaus, *Appl. Phys. Lett.* **79**, 677 (2001).

¹²J. P. Heremans, C. M. Thrush, D. T. Morelli, and M.-C. Wu, *Phys. Rev. Lett.* **88**, 216801 (2002).

¹³D. Li, A. L. Prieto, Y. Wu, M. M. Gonzalez, A. M. Stacy, T. Sands, R. Gronsky, P. Yang, and A. Majumdar, *Proc. 21st Intl. Conf. Thermoelectrics*, Long Beach, CA, 25–29 August 2002, p. 333.

¹⁴C. Jin, X. Xiang, C. Jia, W. Liu, W. Cai, L. Yao, and X. Li, *J. Phys. Chem. B* **108**, 1844 (2004).

¹⁵L. Shi, D. Li, C. Yu, W. Jang, D. Kim, Z. Yao, P. Kim, and A. Majumdar, *J. Heat Transfer* **125**, 881 (2003).

¹⁶S. B. Cronin, Y. Lin, O. Rabin, M. R. Black, J. Y. Ying, M. S. Dresselhaus, P. L. Gai, J. P. Minet, and J. P. Issi, *Nanotechnology* **13**, 653 (2002).

¹⁷J. P. Fleurial, L. Gaillard, R. Triboulet, H. Scherrer, and S. Scherrer, *J. Phys. Chem. Solids* **49**, 1237 (1988).

¹⁸C. B. Satterthwaite and R. W. Ure, Jr., *Phys. Rev.* **108**, 1164 (1957).